COMPUTER VISION, GRAPHICS, AND IMAGE PROCESSING 39, 226–245 (1987)

Design and Implementation of a Colour Vision Model for Computer Vision Applications

FEDERICO BUMBACA

Laboratory for Intelligent Systems, Division of Electrical Engineering, National Research Council of Canada, Montreal Road, Ottawa K1A 0R8, Canada

AND

KENNETH C. SMITH

Department of Electrical Engineering, University of Toronto, Toronto M5S 1A4, Canada

Received January 23, 1986; accepted September 8, 1986

In the past, the area of computer vision has predominantly dealt with the processing of either binary or grey-scale images with little emphasis placed on colour. A colour vision model is therefore developed and implemented for computer vision applications. The coordinate system utilized, however, is of paramount importance since all subsequent processing depends on its appropriateness to the problem domain, namely computer vision. To this end, it is argued that a suitable perceptual coordinate system may be found by investigating properties of the human visual system. Experimental data is employed to optimize the parameters of a model of the human system as well as to determine its performance. The coordinate system which follows from this model is also related to the internationally accepted CIE colour system.

1. INTRODUCTION

In the past, the area of computer vision has predominantly dealt with the processing of either binary or grey-scale images, with little emphasis placed on colour. Although several researchers [1–6, 20] have brushed upon this new challenge, a well thought out and appropriate coordinate system upon which to base any substantial effort does not seem to exist. It is felt that a clue to a suitable coordinate system may be found by investigating the human visual system, yet none of the current coordinate systems found in the literature [1, 14] seem to be intricately related to it. Faugeras [7] has developed a model or coordinate system which may be used for colour image processing but he does not make any mention of its applicability to computer vision problems in general.

As human beings, we intuitively feel that colour is an important part of our visual experience and is useful for powerful visual processing. Would it not then seem reasonable that in order to attempt to reach the capabilities of our own visual system, that computer vision systems be adopted from the human system? In order to capture colour as perceived by the human system is it not at least necessary that a computer system adopt a similar coordinate system? The objective of this paper is to extend the initial idea proposed by Faugeras by developing an improved colour coordinate system based on a simplified view of the human visual system. It is argued, however, that although this model may have certain advantages in digital image processing, emphasis is placed towards its applicability to computer vision. It is beyond the scope of this paper to demonstrate fully that this approach lies in the direction of eventually building systems which will be able to understand images as

0734-189X/87 $3.00

the human observer does, and it is hoped that this concept is intuitive. For example, it is possible that the colour codes on electronic components such as resistors may have been chosen by humans through our visual system to present distinct codes represented by colours which should be as perceptually distant from each other as possible. Therefore, in order for a digital system to equally map these colours into a coordinate system which spaces them apart in the same manner as the human visual system, the coordinate system should be similar to that of the human visual system. It may be further argued that a coordinate system based on the human system is better at discriminating between colours, as we recognize them, than one which is not, and since colour (or intensity) discrimination is vital to any computer vision algorithm, it would seem logical that a coordinate system which provides a basis for efficient discrimination would be beneficial [4].

Due to the complexity of human colour perception this paper only attempts to capture a few of its principles and does not in any way represent a complete model of the human visual system. The theories discussed are basically point theories, which do not account for such phenomena as spatial and temporal chromatic adaptation.

As computer vision research finds its way out of universities and research laboratories into the industrial environment there is increasing pressure to strive towards some type of global standardization in industrial colour measurement. To ensure cooperative progress, the coordinate system used by a colour vision system should be simply related to or derived from an internationally accepted standard. The system proposed by the Commission Internationale de l'Eclairage (CIE) has been adopted here and it is shown to be related to the cone sensitivity functions of the eye by Smith and Pokorny [11].

2. BACKGROUND

2.1. Colorimetry

The experimental laws of colour-matching state that over a wide range of conditions of observation, colours can be matched by additive mixtures of three fixed primary colours. These primaries must be such that none of them can be matched by a mixture of the other two. Furthermore those matches are linear over a wide range of observing conditions which implies two facts. First, the match between two colours continues to hold if the corresponding stimuli are increased or reduced by the same amount, their respective relative spectral energy distributions being unchanged. Second, if colours C and D match and colours E and F match, then the additive mixture of colours C and E matches the corresponding additive mixture of colours D and F.

Colours can therefore be represented by three-dimensional vectors whereas colour matches can be represented by linear equations between such vectors. If $\mathbf{C}$ represents a given colour and $\mathbf{R}, \mathbf{G}, \mathbf{B}$ represent unit amounts of three fixed primaries then the equation

$$\mathbf{C} = R\mathbf{R} + G\mathbf{G} + B\mathbf{B}, \qquad \text{where } R \geq 0,\ G \geq 0,\ B \geq 0 \tag{1}$$

expresses the fact that the given colour is matched by an additive mixture of quantities R, G, B, respectively, of the given primaries. R, G, B are called the

tristimulus values of the given colour in the particular set of primaries used. Another set of important quantities is the chromaticity coordinates r, g, b defined by

$$r = \frac{R}{R + G + B} \tag{2}$$

$$g = \frac{G}{R + G + B} \tag{3}$$

$$b = \frac{B}{R + G + B}. \tag{4}$$

The linearity property also allows us to define completely the colour-matching properties of the observing eye in the given primary system by three functions of wavelength $r(\lambda)$, $g(\lambda)$, $b(\lambda)$ called colour-matching functions. If the colour C has a spectral energy distribution $p(\lambda)$ then its tristimulus values are

$$R = \int p(\lambda) r(\lambda)\, d\lambda \tag{5}$$

$$G = \int p(\lambda) g(\lambda)\, d\lambda \tag{6}$$

$$B = \int p(\lambda) b(\lambda)\, d\lambda, \tag{7}$$

where the integrals are taken over the visible spectrum. In additive colour-matching experiments, colours C_1 and C_2 of spectral energy distributions $p_1(\lambda)$ and $p_2(\lambda)$ match if and only if

$$\int p_1(\lambda) r(\lambda)\, d\lambda = \int p_2(\lambda) r(\lambda)\, d\lambda \tag{8}$$

$$\int p_1(\lambda) g(\lambda)\, d\lambda = \int p_2(\lambda) g(\lambda)\, d\lambda \tag{9}$$

$$\int p_1(\lambda) b(\lambda)\, d\lambda = \int p_2(\lambda) b(\lambda)\, d\lambda. \tag{10}$$

In the case of physical object colours, the properties of the illuminant and the object surface reflectance become critical [16]. Land [16] has demonstrated that under certain conditions colour matches may be attained without satisfying (8)–(10) and that (8)–(10) do not always lead to colour matches. His experiments, however, deal with varying illuminants between the two object colours being matched as well as varying surrounds. Judd [21–22] discusses some of Land's phenomena and explains them using traditional arguments. Land's observations are based on a concept of Helmholtz; that is, in judging the colour of objects in a real scene, we make an allowance for the colour of the illuminant. In other words, if the viewer knows certain objects in the picture to be white under "normal" conditions of illumination, then the eye and brain effect an inevitable and unconscious colour transformation that makes this true. Another explanation of Land's results is based

on simultaneous contrast and chromatic adaptation. In this paper, the same illuminant is utilized throughout and the surrounds of the object colours are ignored due to the point theory the model assumes of the human visual system. Additionally, the colour-matching experiments to be cited in the paper are not affected by illumination (due to the nature of the experiments) and are also based on constant surrounds, thereby avoiding the effects observed by Land. It may then be said that (11)–(13) are equivalent to (8)–(10) but deal with object colour matches as opposed to additive colour matches

$$\int \rho_1(\lambda)\mathrm{S}(\lambda)r(\lambda)\,d\lambda = \int \rho_2(\lambda)\mathrm{S}(\lambda)r(\lambda)\,d\lambda \tag{11}$$

$$\int \rho_1(\lambda)\mathrm{S}(\lambda)g(\lambda)\,d\lambda = \int \rho_2(\lambda)\mathrm{S}(\lambda)g(\lambda)\,d\lambda \tag{12}$$

$$\int \rho_1(\lambda)\mathrm{S}(\lambda)b(\lambda)\,d\lambda = \int \rho_2(\lambda)\mathrm{S}(\lambda)b(\lambda)\,d\lambda, \tag{13}$$

where $\rho_1(\lambda)$ and $\rho_2(\lambda)$ are the spectral reflectance functions of the surface materials and $\mathrm{S}(\lambda)$ is the spectral energy distribution of the illuminant. It is argued that (11)–(13) are valid for the conditions imposed on the experiments discussed in this paper and show an equal correspondence to (8)–(10) and the additive colour-matching experiments. These equations are also in agreement with Land's retinex theory [16] since a match is made when the reflectivities of the two surfaces match for a given illuminant.

We may also describe a change of primaries as a simple matrix multiplication operation whereby the new tristimulus values L, M, S of a given colour and the new colour-matching functions $l(\lambda)$, $m(\lambda)$, $s(\lambda)$ are given by

$$\mathbf{T}_n = A\mathbf{T}_0 \tag{14}$$

$$\mathbf{t}_n = A\mathbf{t}_0, \tag{15}$$

where $\mathbf{T}_n = [\mathrm{L}, \mathrm{M}, \mathrm{S}]^t$, $\mathbf{T}_0 = [R, G, B]^t$, $\mathbf{t}_n = [l(\lambda), m(\lambda), s(\lambda)]^t$, $\mathbf{t}_0 = [r(\lambda), g(\lambda), b(\lambda)]^t$, and A is a three-by-three matrix whose rows are the tristimulus values of the new primaries in the system of the old primaries.

A standard observer has been developed in 1931 by the CIE, whose colour-matching functions are denoted by $x(\lambda)$, $y(\lambda)$, $z(\lambda)$ and shown in Fig. 1. The matches predicted with their aid using (8)–(10) represent average matches for humans with normal colour vision as opposed to humans with any one of the several forms of colour blind vision. A more detailed introduction to colorimetry may be found in [8].

2.2. Psychophysics of the Human Visual System

The physiological basis of trichromatic colour matches is the linear absorption of light at photopic levels of illumination (when the effect of rod receptors is negligible) by three types of cone receptors in the human fovea [7]. However, specification of the spectral absorption characteristics of the three different cone types has been difficult since it has not been possible to extract cone pigments from the eyes of primates [9]. A number of different approaches has been taken to yield this information which is essential to understanding colour vision. All these approaches agree on two points. First, there are three types of cones with their absorption

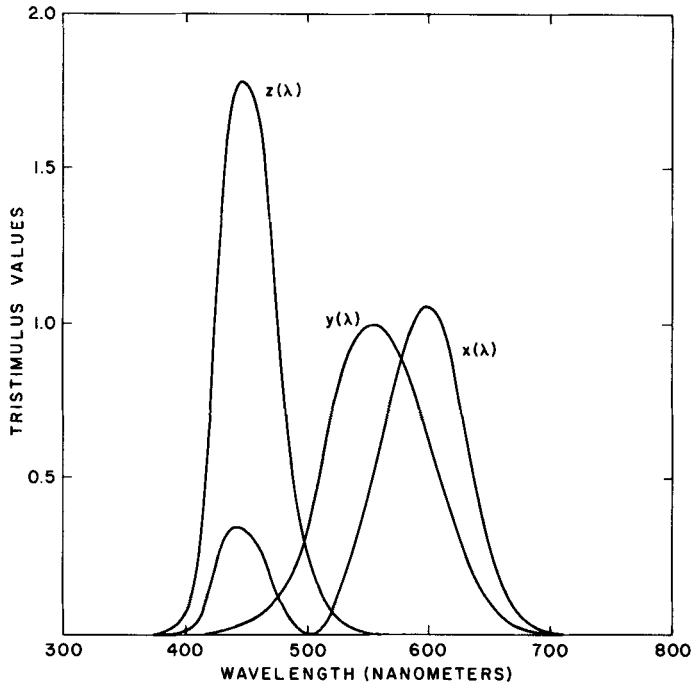

FIG. 1. Colour-matching functions $x(\lambda)$, $y(\lambda)$, and $z(\lambda)$.

curves peaking at about 445, 540, and 570 nm. Second, these absorptions curves are quite abroad and fit to a first approximation the Dartnall nomogram [10].

The terms L-cones (containing the long-wavelength peaking pigment), M-cones (containing the medium-wavelength peaking pigment) and S cones (containing the short-wavelength peaking pigment) will be used to denote the cone types containing the 570, 540, and 445 nm peaking pigments, respectively [7].

Physiological studies have shown that the activity or response of the cone receptors is proportional not to the intensity of the stimulus but rather to its logarithm [7]. This idea is supported by Fechner's law, which states that the just-noticeable brightness difference is proportional to the logarithm of the stimulus intensity.

Further results obtained by neurophysiological experiments on lateral geniculate nucleus (LGN) cells of primates are now summarized [17–19]. Four types of spectrally opponent cells exist in the LGN, a part of the brain to which the retina projects itself. They showed excitation to some wavelengths and inhibition to others when the eye was stimulated with flashes of monochromatic lights. The cells whose response showed maximum excitation around 500 nm and maximum inhibition around 630 nm were called green excitatory, red inhibitory (+G − R). Other cells showing opposite responses were called red excitatory, green inhibitory cells (+R − G). The cells showing maximum excitation (inhibition) at 600 nm and maximum inhibition (excitation) at 440 nm were called yellow excitatory, blue inhibitory cells (+Y − B) and blue excitatory, yellow inhibitory (+B − Y), respectively.

In addition to these four varieties of spectrally opponent cells, two other classes of cells were found that did not give spectrally opponent responses but rather responded in the same direction to lights of all wavelengths. Those cells, which are not involved with colour vision, are called white excitatory, black inhibitory cells (+Wh − Bl) and black excitatory, white inhibitory cells (+Bl − Wh).

Evidence also exists in favor of the assumption of separate chromatic and achromatic channels, each gaining its information from the same receptors but processing it in different ways. Spectrally non-opponent cells which correspond to the achromatic channel add together the (Log) outputs of the L- and M-cones (and possibly S-cones as well). Spectrally opponent cells which correspond to the chromatic channels subtract the (Log) outputs of the L- and M-cones for the red–green system, of the L- and S-cones for the yellow–blue system.

3. A COLOUR VISION MODEL

3.1. Psychophysical Approach

As mentioned previously, there are three cone types involved in human photopic (day) vision, each of which contains a pigment with different spectral absorption characteristics. From colour-matching experiments, the CIE derived a set of three colour-matching functions which, according to Grassman laws of colour mixture, have to be a linear combination of the pigment absorption curves. There is an infinite number of such combinations but we are restricted by the fact that the resulting curves should be positive in the visible spectrum and have a single maximum at a wavelength close to the ones indicated previously. Despite these restrictions there are still many of these "fundamentals" in the literature [11].

Faugeras [7] has decided to adopt the fundamentals proposed by Stiles [11]. However, a more recent model proposed by Pokorny and Smith [10] seems to be much more readily acceptable today. This model is in accordance with the idea, proposed by other investigators as well, that the luminous efficiency function of the normal trichromat is mediated only by the red- and green-cone mechanisms and that the blue-cone mechanism makes no contribution to "luminance signals." In other words, a colour blind person or dichromat, lacking in the tritanope or blue relative spectral sensitivity, $s(\lambda)$, perceives luminance information as well as does a trichromat. This statement, together with the fact that the CIE luminous efficiency function, $V(\lambda)$, has values at short wavelengths that are considered excessively low, have prompted us to adopt the Pokorny and Smith fundamentals. It should be mentioned that the CIE luminous efficiency function is, by definition, equal to the CIE curve $y(\lambda)$, and that it has been modified by Judd [11] to take into account its low values at short wavelengths.

The fundamentals of Pokorny and Smith may be related to the CIE curves, $x'(\lambda), y'(\lambda), z'(\lambda)$, which are the Judd modified CIE 1931 standard functions [11], by a matrix transformation

$$\begin{bmatrix} l(\lambda) \\ m(\lambda) \\ s(\lambda) \end{bmatrix} = T \begin{bmatrix} x'(\lambda) \\ y'(\lambda) \\ z'(\lambda) \end{bmatrix}, \qquad \text{where } T = \begin{bmatrix} 0.15514 & 0.54312 & -0.03286 \\ -0.15514 & 0.45684 & 0.03286 \\ 0.0 & 0.0 & 0.00801 \end{bmatrix}. \tag{16}$$

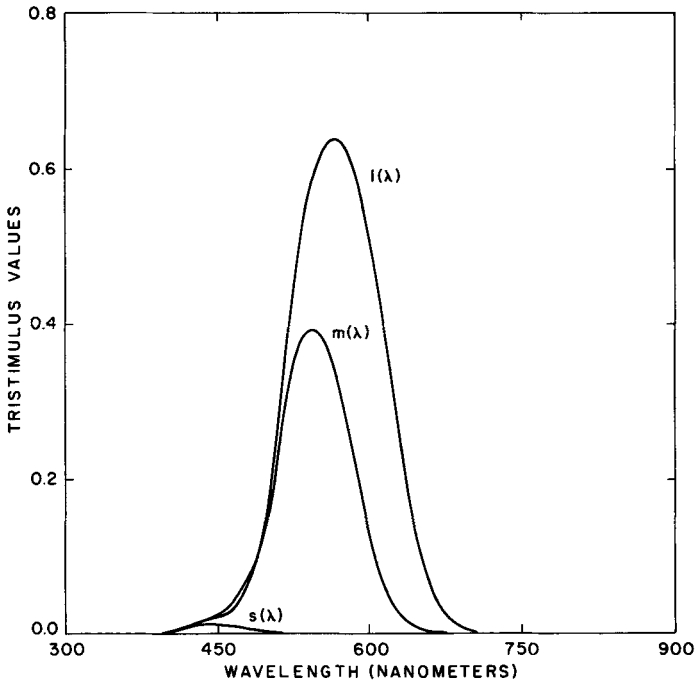

FIG. 2. Absorption curves l(λ), m(λ) and s(λ).

Since the blue-cone mechanism, s(λ), makes no contribution to luminance, (17) also results.

$$V_{\text{mod}}(\lambda) = l(\lambda) + m(\lambda). \tag{17}$$

This constraint on (16) helps to improve the agreement between predicted and observed colour-matching functions of tritanopes. Figure 2 shows the resulting absorption curves l(λ), m(λ), s(λ), which are positive in the visible spectrum and have single maxima at, respectively, 575, 540, and 445 nm.

A precise description, similar to that given by Faugeras [7], of the cone absorption stage of the model may now be presented. Let $I(x, y, \lambda)$ be an image, where x and y are the spatial coordinates and λ is the wavelength of the light. Then the absorption of this light energy by the three pigments yields the three signals

$$\mathrm{L}(x, y) = \int I(x, y, \lambda) l(\lambda)\, d\lambda \tag{18}$$

$$\mathrm{M}(x, y) = \int I(x, y, \lambda) m(\lambda)\, d\lambda \tag{19}$$

$$\mathrm{S}(x, y) = \int I(x, y, \lambda) s(\lambda)\, d\lambda \tag{20}$$

where each integral is taken over the visible spectrum.

The nonlinear response of the cones transforms those signals in the following

way:

$$L^*(x, y) = \text{Log}[L(x, y)] \tag{21}$$

$$M^*(x, y) = \text{Log}[M(x, y)] \tag{22}$$

$$S^*(x, y) = \text{Log}[S(x, y)]. \tag{23}$$

It has been mentioned that there exist separate chromatic and achromatic channels in the human visual path, each gaining its information from the same receptors but processing it in different ways. The achromatic response will be called A and the two chromatic responses will be called C_1 and C_2. Equations (24)–(26) express mathematically the ideas discussed earlier,

$$A = a(\alpha L^* + \beta M^*) = a(\alpha \text{Log} L + \beta \text{Log} M) \tag{24}$$

$$C_1 = u_1(L^* - M^*) = u_1 \text{Log}(L/M) \tag{25}$$

$$C_2 = u_2(L^* - S^*) = u_2 \text{Log}(L/S), \tag{26}$$

where A is a mathematical description of the response of (+Bl − Wh) and (+Wh − Bl) cells which add the Log outputs of the L-cones and M-cones (in agreement with the Pokorny and Smith fundamentals and spectral non-opponent cells). C_1 and C_2 are mathematical descriptions of the responses of (+R − G), (+G − R), and (+B − Y), (+Y − B) cells which subtract the Log outputs of the L- and M-cones and L- and S-cones, respectively (in agreement with the response of spectrally opponent cells).

This model is in agreement with Stockham's model for achromatic vision [12]. For an achromatic image the outputs of the cone absorption stage are by definition equal,

$$L(x, y) = M(x, y) = S(x, y), \tag{27}$$

and thus

$$C_1(x, y) = C_2(x, y) = 0. \tag{28}$$

In that case only the achromatic channel A is active,

$$A = a(\alpha + \beta)L^*(x, y), \tag{29}$$

which is exactly Stockham's model. It may then be stated that A carries the brightness information.

Consider Fig. 3 which describes the colour space spanned by our model. It provides a three-dimensional vector space as a quantitative definition of some perceptually important parameters. If A, brightness, is now considered constant, the relationship of C_1 and C_2 to the perception of hue and saturation may be discussed. For a colour at point Q, saturation is related to the distance Oq while hue is related to the angle θ. Saturation is thus proportional to the sum of the activities in the C_1 and C_2 channels while hue is proportional to the ratio of these activities.

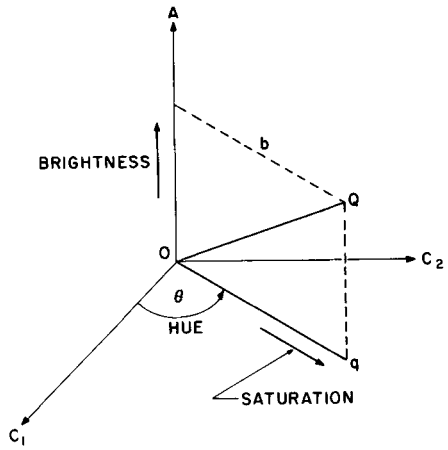

FIG. 3. The AC_1C_2 space.

3.2. Colorimetric Analysis

A line element will now be derived to quantitatively determine perceived colour differences from the properties of the three fundamental colour response systems. Line elements aim to specify pairs of colour stimuli that present a particular perceived colour difference, for example, a just-noticeable difference, by the position and distance apart in tristimulus space of the points representing these stimuli [11]. In ordinary or Euclidean space, the distance ds between two neighboring points p_1 and p_2 whose rectangular coordinates (tristimulus values) are (U_1, U_2, U_3) and $(U_1 + dU_1, U_2 + dU_2, U_3 + dU_3)$ is given by

$$(ds)^2 = (dU_1)^2 + (dU_2)^2 + (dU_3)^2. \tag{30}$$

In AC_1C_2 space this line element may be expressed as

$$(ds)^2 = (dA)^2 + (dC_1)^2 + (dC_2)^2. \tag{31}$$

In other words, the AC_1C_2 space is assumed to be a uniform perceptual space in the sense that at a given point the locus of all points corresponding to a just-noticeable difference in perception (brightness or chromaticity) is a sphere of radius 1 centered at that point. This is approximated by adjusting the values of the parameters a, u_1, u_2, of (24)–(26), to be explained later.

The following Riemannian line element in LMS space is easily derived by substituting (24)–(26) into (31),

$$\begin{aligned}(ds)^2 = {} & (a^2\alpha^2 + u_1^2 + u_2^2)\left[\frac{dL}{L}\right]^2 + (a^2\beta^2 + u_1^2)\left[\frac{dM}{M}\right]^2 + u_2^2\left[\frac{dS}{S}\right]^2 \\ & + 2(a^2\alpha\beta - u_1^2)\left[\frac{dL}{L}\right]\left[\frac{dM}{M}\right] - 2u_2^2\left[\frac{dL}{L}\right]\left[\frac{dS}{S}\right].\end{aligned} \tag{32}$$

This line element is based on theoretical considerations regarding the functioning of the visual mechanism coupled with certain qualitative experimental data. It includes cross-product terms of the cone responses to account for the interdependence of the cone systems, a property that the Stiles line element does not possess. As noted in (32) a number of undefined parameters exist which this inductive line element does not quantify. By minimizing the computed deviations from empirical data the best values for these parameters are determined.

According to Grassman's laws of additive colour mixture it can be shown that the function $V_{\text{mod}}(\lambda)$ should be a linear combination of the cones' spectral absorption curves, as is indeed the case (Pokorny and Smith). Our model should also account for the measurements yielding to the function $V_{\text{mod}}(\lambda)$. One method that may be used to measure this function is called the step by step method [11]. Two juxtaposed monochromatic lights of slightly different wavelengths are viewed and the radiance of one is varied until the total difference between the patches is minimum. The wavelength difference can be made so small that the difference in colour at this minimum setting is barely perceptible. This procedure is repeated step by step along the spectrum.

A relative luminous efficiency function can be derived from our model and (32) by a corresponding procedure explained in [11, 13] and is given by

$$\hat{V}_{\text{mod}}(\lambda) = kl(\lambda)^{\alpha/(\alpha+\beta)} m(\lambda)^{\beta/(\alpha+\beta)}, \tag{33}$$

where k has been adjusted to yield a maximum of 1. The parameters α and β have

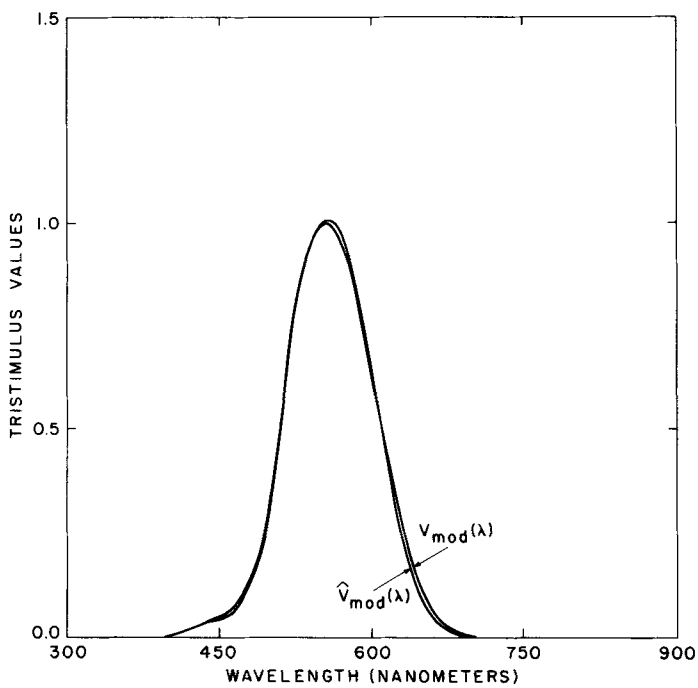

FIG. 4. Luminous efficiency functions $V_{\text{mod}}(\lambda)$ and $\hat{V}_{\text{mod}}(\lambda)$.

been determined such that (17) and (33) are simultaneously satisfied, i.e.,

$$l(\lambda) + m(\lambda) = kl(\lambda)^{\alpha/(\alpha+\beta)} m(\lambda)^{\beta/(\alpha+\beta)}. \tag{34}$$

The optimum values for α and β are 0.7186 and 0.2814, respectively, where $\alpha + \beta = 1$. They produce the best least squares estimate of (34). Figure 4 plots (33) and the true $V_{\text{mod}}(\lambda)$ given by (17). It is quite evident that the two curves are in very good agreement for the entire visible spectrum.

The line element, (32), may also be used to predict the human observer's ability to discriminate between the wavelengths of two just-noticeable different monochromatic stimuli of equal brightness. Utilizing (32) and making appropriate substitutions for dL, dM, dS, L, M, and S in terms of $dl(\lambda)$, $dm(\lambda)$, $ds(\lambda)$, l, m, and s, (35) results. The procedure is also described in [11] and [13].

$$\begin{aligned}
(ds)^2 = (d\lambda)^2 \Bigg\{ & \left(a^2\alpha^2 + u_1^2 + u_2^2\right) \\
& \times \left[\frac{dl(\lambda)}{d\lambda}\frac{1}{l(\lambda)} - \left(\frac{dl(\lambda)}{d\lambda}\frac{\alpha}{l(\lambda)} + \frac{dm(\lambda)}{d\lambda}\frac{\beta}{m(\lambda)}\right)\right]^2 \\
& + \left(a^2\beta^2 + u_1^2\right)\left[\frac{dm(\lambda)}{d\lambda}\frac{1}{m(\lambda)} - \left(\frac{dl(\lambda)}{d\lambda}\frac{\alpha}{l(\lambda)} + \frac{dm(\lambda)}{d\lambda}\frac{\beta}{m(\lambda)}\right)\right]^2 \\
& + u_2^2\left[\frac{ds(\lambda)}{d\lambda}\frac{1}{s(\lambda)} - \left(\frac{dl(\lambda)}{d\lambda}\frac{\alpha}{l(\lambda)} + \frac{dm(\lambda)}{d\lambda}\frac{\beta}{m(\lambda)}\right)\right]^2 \\
& + 2\left(a^2\alpha\beta - u_1^2\right)\left[\frac{dl(\lambda)}{d\lambda}\frac{1}{l(\lambda)} - \left(\frac{dl(\lambda)}{d\lambda}\frac{\alpha}{l(\lambda)} + \frac{dm(\lambda)}{d\lambda}\frac{\beta}{m(\lambda)}\right)\right] \\
& \times \left[\frac{dm(\lambda)}{d\lambda}\frac{1}{m(\lambda)} - \left(\frac{dl(\lambda)}{d\lambda}\frac{\alpha}{l(\lambda)} + \frac{dm(\lambda)}{d\lambda}\frac{\beta}{m(\lambda)}\right)\right] \\
& - 2u_2^2\left[\frac{dl(\lambda)}{d\lambda}\frac{1}{l(\lambda)} - \left(\frac{dl(\lambda)}{d\lambda}\frac{\alpha}{l(\lambda)} + \frac{dm(\lambda)}{d\lambda}\frac{\beta}{m(\lambda)}\right)\right] \\
& \times \left[\frac{ds(\lambda)}{d\lambda}\frac{1}{s(\lambda)} - \left(\frac{dl(\lambda)}{d\lambda}\frac{\alpha}{l(\lambda)} + \frac{dm(\lambda)}{d\lambda}\frac{\beta}{m(\lambda)}\right)\right]\Bigg\}.
\end{aligned} \tag{35}$$

For a sequence of pairs of stimuli spanning the spectrum of all the same small-step brightness (constant ds) determined from the line element, the variation of $d\lambda$ with λ calculated from (35) is compared with the mean experimental data reported by Wright and Pitt [11], as shown in Fig. 5. This comparison must be carefully considered since wavelength discrimination has been studied by many researchers [23], each producing results which vary considerably from the others'

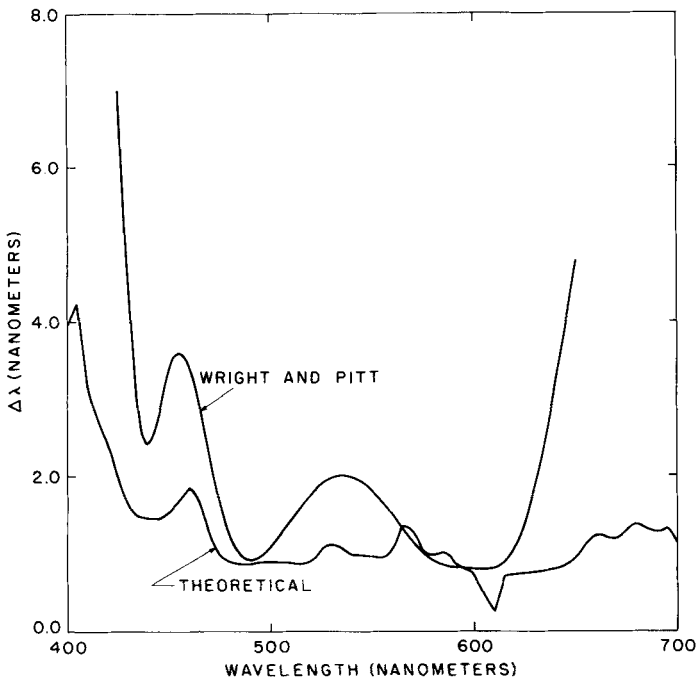

FIG. 5. Wavelength discrimination.

results. However, the data reported by Wright and Pitt seem to exhibit the features most commonly observed.

The line element given in (32) may also be expressed in terms of CIE (x, y) chromaticity coordinates and luminance, Y, through

$$\begin{bmatrix} l(\lambda) \\ m(\lambda) \\ s(\lambda) \end{bmatrix} = \begin{bmatrix} t_{11} & t_{12} & t_{13} \\ t_{21} & t_{22} & t_{23} \\ t_{31} & t_{32} & t_{33} \end{bmatrix} \begin{bmatrix} x(\lambda) \\ y(\lambda) \\ z(\lambda) \end{bmatrix},$$

where

$$T = \begin{bmatrix} 0.1195 & 0.5494 & -2.429 \times 10^{-2} \\ -0.1361 & 0.4348 & 3.025 \times 10^{-2} \\ 1.250 \times 10^{-5} & -1.049 \times 10^{-5} & 7.227 \times 10^{-3} \end{bmatrix}, \tag{36}$$

where T is obtained by minimizing the least squares errors between the approximation obtained by (36) and the true $l(\lambda), m(\lambda), s(\lambda)$ functions. Substituting this

transformation into (32) determines the desired line element expressed by

$$
\begin{aligned}
(ds)^2 = (dx)^2 \Bigg\{ & \left(a^2\alpha^2 + u_1^2 + u_2^2\right)\left(\frac{p_{11}}{\mathrm{L}}\right)^2 + \left(a^2\beta^2 + u_1^2\right)\left(\frac{p_{21}}{\mathrm{M}}\right)^2 + u_2^2\left(\frac{p_{31}}{\mathrm{S}}\right)^2 \\
& + 2\left(a^2\alpha\beta - u_1^2\right)\left(\frac{p_{11}}{\mathrm{L}}\right)\left(\frac{p_{21}}{\mathrm{M}}\right) - 2u_2^2\left(\frac{p_{11}}{\mathrm{L}}\right)\left(\frac{p_{31}}{\mathrm{S}}\right)\Bigg\} \\
& + dx\,dy\Bigg\{\left(a^2\alpha^2 + u_1^2 + u_2^2\right)\left(\frac{p_{11}p_{12}}{\mathrm{L}^2}\right) + \left(a^2\beta^2 + u_1^2\right)\left(\frac{p_{21}p_{22}}{\mathrm{M}^2}\right) \\
& + u_2^2\left(\frac{p_{31}p_{32}}{\mathrm{S}^2}\right) + \left(a^2\alpha\beta - u_1^2\right)\left(\frac{p_{11}p_{22} + p_{12}p_{21}}{\mathrm{LM}}\right) - u_2^2\left(\frac{p_{11}p_{32} + p_{12}p_{31}}{\mathrm{LS}}\right)\Bigg\} \\
& + (dy)^2\Bigg\{\left(a^2\alpha^2 + u_1^2 + u_2^2\right)\left(\frac{p_{12}}{\mathrm{L}}\right)^2 + \left(a^2\beta^2 + u_1^2\right)\left(\frac{p_{22}}{\mathrm{M}}\right)^2 \\
& + u_2^2\left(\frac{p_{32}}{\mathrm{S}}\right)^2 + 2\left(a^2\alpha\beta - u_1^2\right)\left(\frac{p_{12}}{\mathrm{L}}\right)\left(\frac{p_{22}}{\mathrm{M}}\right) - 2u_2^2\left(\frac{p_{12}}{\mathrm{L}}\right)\left(\frac{p_{32}}{\mathrm{S}}\right)\Bigg\}, \qquad (37)
\end{aligned}
$$

where

$$
\begin{aligned}
p_{11} &= \frac{Y}{y}(t_{11} - t_{13}) \\
p_{12} &= \frac{Y}{y^2}\left[x(t_{13} - t_{11}) - t_{13}\right] \\
p_{21} &= \frac{Y}{y}(t_{21} - t_{23}) \\
p_{22} &= \frac{Y}{y^2}\left[x(t_{23} - t_{21}) - t_{23}\right] \\
p_{31} &= \frac{Y}{y}(t_{31} - t_{33}) \\
p_{32} &= \frac{Y}{y^2}\left[x(t_{33} - t_{31}) - t_{33}\right].
\end{aligned}
$$

Equation (37) may be used to compute loci of constant dss around given points of chromaticity (x, y) for a constant level of luminance Y. Such loci are ellipses in the chromaticity diagram and circles in C_1C_2 space. If the positions of the given chromaticity points are appropriately chosen, a direct comparison of the computed ellipses with those measured by MacAdam [11] can be made. It is assumed that chromaticity and brightness errors are independent, enabling us to optimize a and u_1u_2 independently. The optimization procedure for a is based on work by Brown and MacAdam [15] and is detailed in [7]. Optimization of parameters u_1u_2 is performed by mapping MacAdam's ellipses into C_1C_2 space (24)–(26) and then computing the values for u_1u_2 which result in their least squares best fit with circles of radius $\frac{1}{3}$ [7, 13]. Figures 6 and 7 give plots of MacAdam's 25 ellipses and the

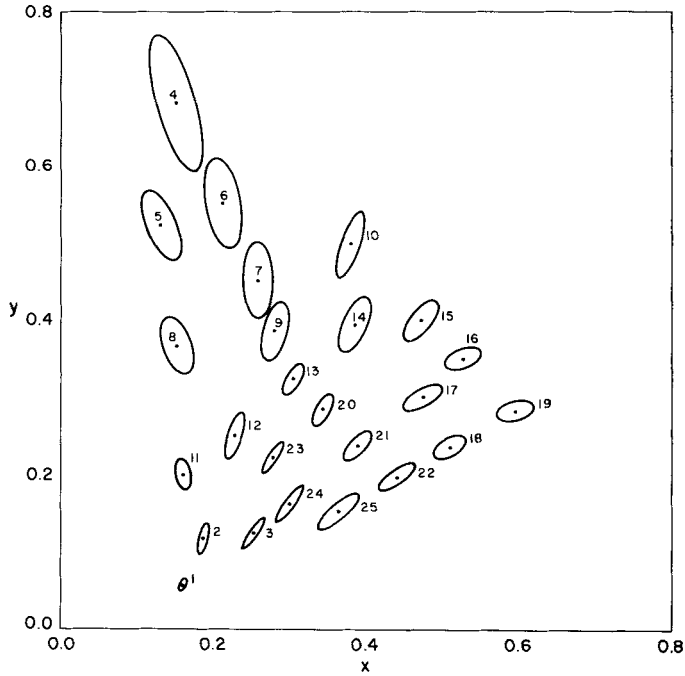

FIG. 6. MacAdam ellipses in CIE space.

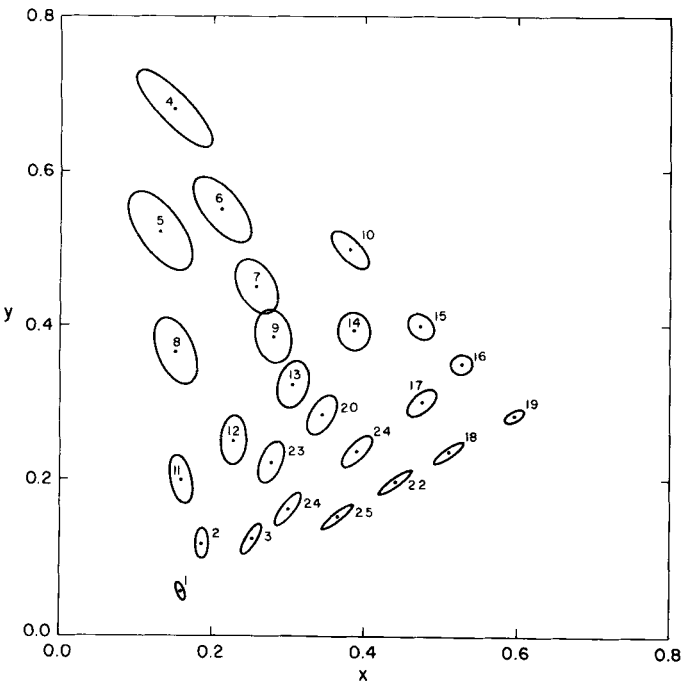

FIG. 7. Predicted ellipses in CIE space.

corresponding ellipses predicted by the line element, respectively. There is a general similarity between the two sets of ellipses. The orientations of the ellipses correspond well, and their areas also show a reasonable correlation. The optimized values for a, u_1, u_2 are 22.6, 41.6 and 10.5, respectively.

Luo and Rigg [24] have recently computed the chromaticity-discrimination ellipses for surface colours and provide an interesting discussion of their results. Due to the various errors in their original data, these ellipses were not used for the optimization discussed above.

4. MODEL IMPLEMENTATION

The previous description and analysis of the colour model on which the system is to be based is only a theoretical one without any reference to practical considerations. The success or failure of the model is critically linked to the realizability of the CIE curves or cone sensitivity functions.

It has been decided to implement the CIE curves from which the LMS and AC_1C_2 coordinates may be obtained. Due to the high cost of having the $x(\lambda)$, $y(\lambda)$, $z(\lambda)$ filters made for our particular vidicon camera a set of four standard filters have been purchased which approximate the desired responses. Two Kodak Wratten filters, f47 and f98, are used to approximate the $z(\lambda)$ and short wavelength part of the $x(\lambda)$ curves. They will be referred to as $b(\lambda)$ and $r_1(\lambda)$, respectively. Two additional Schott glass filters, VG9 and OG55, are used to approximate $y(\lambda)$ and the long wavelength part of the $x(\lambda)$ curves, to be referred to as $g(\lambda)$ and $r_2(\lambda)$, respectively. The camera response must also be taken into account. It should be noted that all of the aforementioned filters and the camera's spectral response are quite sensitive in the near infrared region. This is not an acceptable characteristic since none of the CIE curves have this property. An infrared absorbing filter from Schott, KG5, has therefore been used to eliminate this unwanted light. The resulting (r_1, r_2, g, b) curves after adjusting for the camera response and the infrared filtering are plotted in Fig. 8.

A linear transformation from R_1R_2GB space to XYZ space is now required and expressed by

$$x(\lambda) = m_{11}r_1(\lambda) + m_{12}r_2(\lambda) + m_{13}g(\lambda) + m_{14}b(\lambda) \tag{38}$$

$$x(\lambda) = m_{21}r_1(\lambda) + m_{22}r_2(\lambda) + m_{23}g(\lambda) + m_{24}b(\lambda) \tag{39}$$

$$x(\lambda) = m_{31}r_1(\lambda) + m_{32}r_2(\lambda) + m_{33}g(\lambda) + m_{34}b(\lambda), \tag{40}$$

where m_{ij} are constants. Multiplying both sides by $p(\lambda)$, the spectral energy distribution of the source, and integrating over the wavelength limits yields

$$\begin{bmatrix} X \\ Y \\ Z \end{bmatrix} = \begin{bmatrix} m_{11} & m_{12} & m_{13} & m_{14} \\ m_{21} & m_{22} & m_{23} & m_{24} \\ m_{31} & m_{32} & m_{33} & m_{34} \end{bmatrix} \begin{bmatrix} \mathrm{R}_1 \\ \mathrm{R}_2 \\ \mathrm{G} \\ \mathrm{B} \end{bmatrix}. \tag{41}$$

Pratt [14] suggests two strategies for determining the estimated tristimulus values XYZ for the sensor signals $\mathrm{R}_1\mathrm{R}_2\mathrm{GB}$. One approach, method one, is to select four key colours and then compute the coefficients m_{ij} that result in exact colorimetric

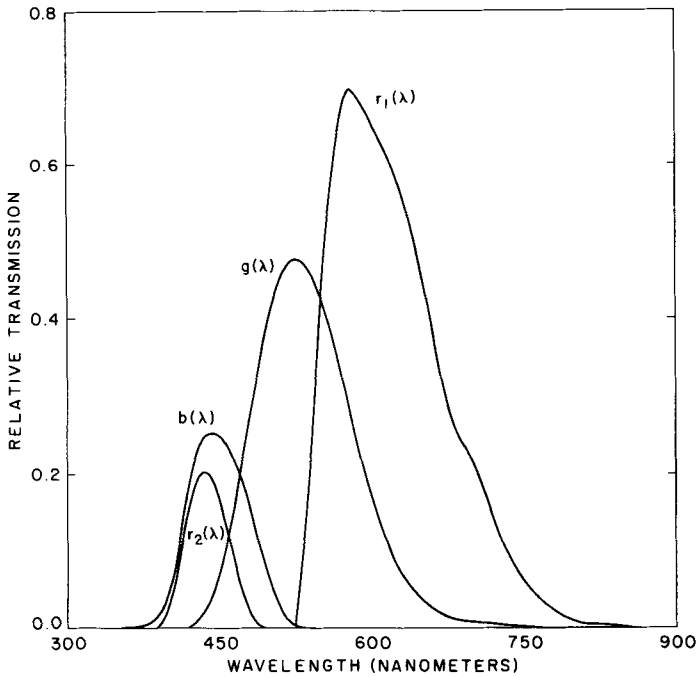

FIG. 8. Spectral characteristics of $r_1 r_2 gb$ appropriate adjustments.

reproduction of the key colours. Then, hopefully, any other arbitrary colour will not depart substantially from its true colorimetric values. The colours that are generally reproduced with the greatest error in chromaticity are the highly saturated colours. Therefore with saturated test colours C_i of known tristimulus values $R_{1i}R_{2i}G_iB_i$ and $X_iY_iZ_i$, four matrix equations are formed,

$$\begin{bmatrix} X_i \\ Y_i \\ Z_i \end{bmatrix} = \begin{bmatrix} m_{11} & m_{12} & m_{13} & m_{14} \\ m_{21} & m_{22} & m_{23} & m_{24} \\ m_{31} & m_{32} & m_{33} & m_{34} \end{bmatrix} \begin{bmatrix} R_{1i} \\ R_{2i} \\ G_i \\ B_i \end{bmatrix}, \qquad i = 1,2,3,4. \tag{42}$$

Equation (42) may then be solved simultaneously for the coefficients m_{ij}.

Four calibration tiles of the three primary colours, red, green, blue, as well as grey have been used for this purpose. Through numerical methods, the reflectivities of the tiles without the effect of an illuminant as well as a tungsten lamp at a temperature of 3400°K have been computed. It was decided to use this lamp as the source for the system since illuminant D_{65} could not be practically implemented and illuminant A lacks in power at short wavelengths and has a great deal of power at long wavelengths.

After numerically computing the XYZ tristimulus values of the four tiles as well as its R_1R_2GB coordinates with the tungsten lamp as the illuminant, (42) are solved yielding the matrix M. It was noted that this method is very sensitive to noise since

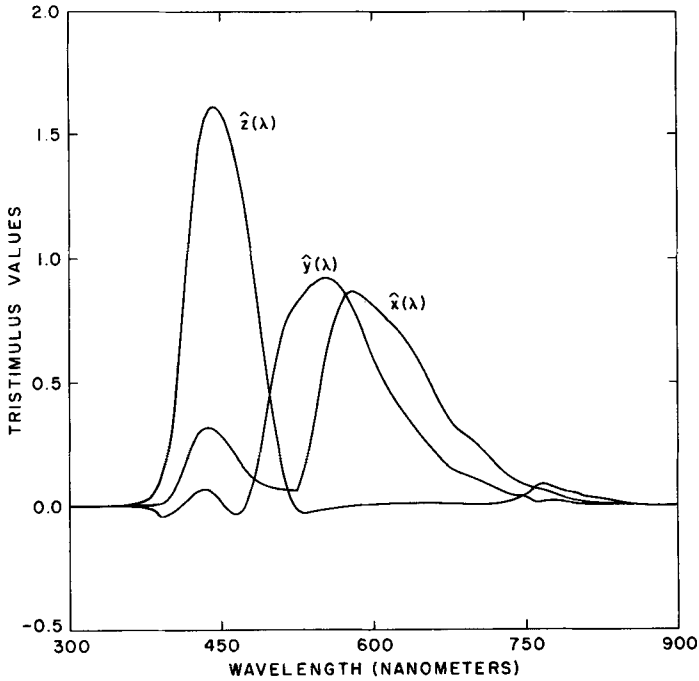

FIG. 9. Approximation to CIE functions $x(\lambda)$, $y(\lambda)$, and $z(\lambda)$.

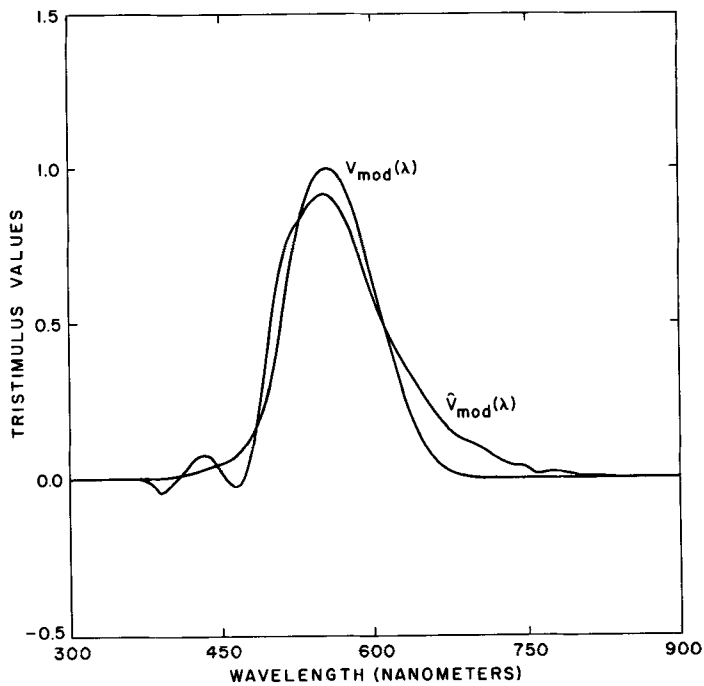

FIG. 10. $\hat{V}_{mod}(\lambda)$ derived from $\hat{l}(\lambda)$, $\hat{m}(\lambda)$, and $\hat{s}(\lambda)$.

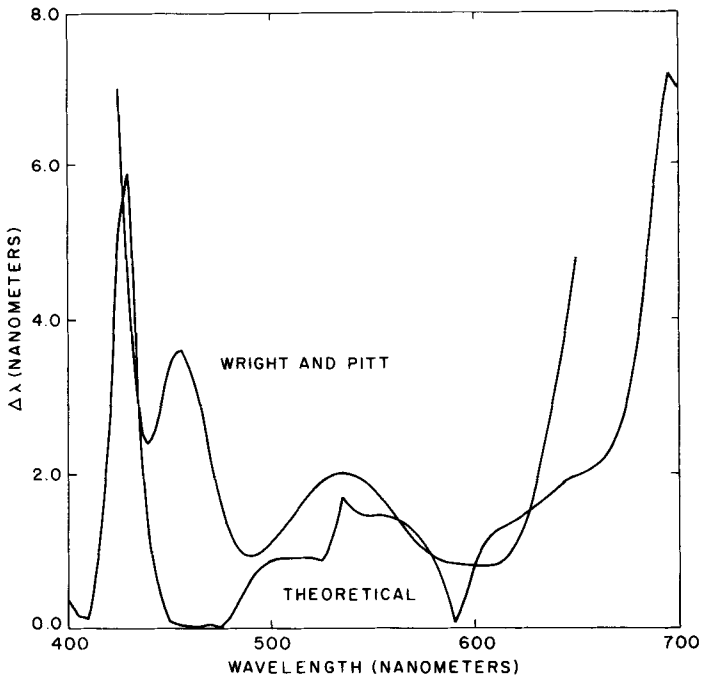

FIG. 11. Wavelength discrimination.

an incorrect value for one of the tristimulus values can produce quite erroneous results.

Another approach, method two, to the estimation of tristimulus values is to select elements of the transformation matrix M to minimize the mean-square errors of $\hat{x}(\lambda) - x(\lambda)$, $\hat{y}(\lambda) - y(\lambda)$, and $\hat{z}(\lambda) - z(\lambda)$ for all wavelengths. $\hat{x}(\lambda)$, $\hat{y}(\lambda)$, and $\hat{z}(\lambda)$ are the approximated CIE functions estimated by (38)–(40). The resulting matrix M (Eq. (43)) produces very good results when compared to the previous method and are plotted in Fig. 9,

$$M = \begin{bmatrix} 1.198 \times 10^{-2} & 1.106 \times 10^{-2} & 1.263 \times 10^{-3} & 3.593 \times 10^{-3} \\ 4.480 \times 10^{-3} & 3.771 \times 10^{-2} & 1.733 \times 10^{-2} & -2.955 \times 10^{-2} \\ 2.348 \times 10^{-4} & 1.892 \times 10^{-4} & -7.112 \times 10^{-4} & 6.380 \times 10^{-2} \end{bmatrix}. \quad (43)$$

These approximation affect the colour vision model as well as its predictions. Figure 10 compares the true luminous efficiency function with that predicted using the approximations to $x(\lambda)$, $y(\lambda)$, and $z(\lambda)$. The new values for α and β are 0.6782 and 0.3218, respectively. Figure 11 compares the data reported by Wright and Pitt with that predicted by the approximation, in terms of wavelength discrimination for a constant small-step brightness. As noted by these plots the model has been significantly disrupted although it is still crudely consistent with experimental observations.

5. CONCLUSIONS

A colour vision model based on physiological observations has been proposed, from which an inductive line element has been derived. This model was then optimized to be consistent with empirical data based on actual experimental results. A thorough analysis has also been conducted from both psychophysical and colorimetry points of view, yielding satisfactory results. The model provides a coordinate system suitable for computer vision applications since it is based on a simplified view of the human visual system and its consequent colour discrimination abilities. In its implementation, however, its performance has been somewhat degraded but may still be considered crudely consistent with experimental data. A complete computer vision system utilizing this model has been implemented in [13] and is shown to perform well.

ACKNOWLEDGMENTS

The authors would like to express their gratitude to Dr. A. R. Robertson of the National Research Council for his many helpful comments and suggestions. This work has been financially supported by a Natural Sciences and Engineering Research Council postgraduate scholarship and Operating Grant A1753.

REFERENCES

1. D. Ballard and C. Brown, *Computer Vision*, Prentice-Hall, Englewood Cliffs, NJ, 1982.
2. J. Chassey and C. Garbay, Iterative process for colour image segmentation using a convexity criterion, SPIE, Vol. 397, pp. 165–172, Applications of Digital Image Processing, 1983.
3. R. Nevatia, A color edge detector and its use in scene segmentation, *IEEE Trans. Systems Man Cybernet.* **7**, 1977, 818–826.
4. Y. Ohta, T. Kanade, and T. Sakai, Color information for region segmentation, *Comput. Graphics Image Process.* **13**, 1980, 222–241.
5. G. S. Robinson, Color edge detection, SPIE Vol. 87, pp. 126–133, Advances in Image Transmission Techniques, 1976.
6. J. M. Rubin and W. A. Richards, *Color Vision and Image Intensities: When Are Changes Material?* A.I. Memo No. 631, Massachusetts Institute of Technology, Artificial Intelligence Laboratory, May 1981.
7. O. Faugeras, *Digital Color Image Processing and Psychophysics within the Framework of a Human Visual Model*, Ph.D. dissertation, University of Utah, June 1976.
8. W. Sproson, *Colour Science in Television and Display Systems*, pp. 96–97, Hilger, Bristol, 1983.
9. R. L. DeValois, Central mechanisms of colour vision, in *Handbook of Sensory Physiology*, Vol. VII/3, *Central Processing of Visual Information A*, pp. 200–253, Springer-Verlag, Berlin/New York, 1973.
10. R. Boynton, *Human Color Vision*, pp. 149–155, 404, Holt, Rinehart & Winston, New York, 1979.
11. G. Wyszecki and W. S. Stiles, *Color Science*, Wiley, New York, 1982.
12. T. G. Stockham JR., Image processing in the context of a visual model, *Proc. IEEE* **60**, 1972, 828–842.
13. F. Bumbaca, *A Real-Time Colour Computer Vision System*, M.A.Sc: thesis, University of Toronto, April 1985.
14. W. Pratt, *Digital Image Processing*, Wiley, Toronto, 1978.
15. W. R. J. Brown and D. L. MacAdam, Visual sensitivities to combined chromaticity and luminance differences, *J. Opt. Soc. Amer.* **39** (1949), 808–834.
16. E. H. Land, The retinex theory of color vision, *Scientific American*, December 1977, 108–128.
17. R. L. DeValois, C. J. Smith, S. T. Kital, and A. J. Karchy, Responses of single cells in different layers of the primate lateral geniculate nucleus to monochromatic light, *Science* **127**, 1958, 238–239.
18. R. L. DeValois, I. Abraman, and G. H. Jacobs, Analysis of response patterns of LGN cells, *J. Opt. Soc. Amer.* **56**, 1966, 966–977.
19. T. N. Wiesel and D. H. Hubel, Spatial and chromatic interactions in the lateral geniculate body of the rhesus monkey, *J. Neurophysiol.* **29**, 1966, 1115–1156.

20. S. DiZenzo, A note on the gradient of a multi-image, *Comput. Vision Graphics Image Process.* **33** 1986, 116–125.
21. D. B. Judd, Hue, saturation and lightness of surface colours with chromatic illumination, *J. Opt. Soc. Amer.*, **30**, 1940, 2–32.
22. D. B. Judd, Appraisal of Land's work on two-primary color projections, *J. Opt. Soc. Amer.* **50**, 1960, 254.
23. J. J. Vos, P. L. Walraven, Analytical description of line element in zone-fluctuation model of colour vision. 1. Basic concepts, *Vision Res.* **12**, 1972, 1327–1343.
24. M. R. Luo, B. Rigg, Chromaticity-discrimination ellipses for surface colours, *COLOR Res. Appli.* **11**, 1986, 25–42.